



HAL
open science

Numerical simulation of in vivo indentation tests: determination of the mechanical properties of human skin

Marie-Angèle Abellan, Eric Feulvarch, Hassan Zahouani, Jean-Michel
Bergheau

► To cite this version:

Marie-Angèle Abellan, Eric Feulvarch, Hassan Zahouani, Jean-Michel Bergheau. Numerical simulation of in vivo indentation tests: determination of the mechanical properties of human skin. CFM 2013 - 21ème Congrès Français de Mécanique, Aug 2013, Bordeaux, France. hal-03440527

HAL Id: hal-03440527

<https://hal.science/hal-03440527>

Submitted on 22 Nov 2021

HAL is a multi-disciplinary open access archive for the deposit and dissemination of scientific research documents, whether they are published or not. The documents may come from teaching and research institutions in France or abroad, or from public or private research centers.

L'archive ouverte pluridisciplinaire **HAL**, est destinée au dépôt et à la diffusion de documents scientifiques de niveau recherche, publiés ou non, émanant des établissements d'enseignement et de recherche français ou étrangers, des laboratoires publics ou privés.

Numerical simulation of in vivo indentation tests: determination of the mechanical properties of human skin

M.-A. ABELLAN^a, E. FEULVARCH^a, H. ZAHOUANI^a, J.-M. BERGHEAU^a

a. Université de Lyon, ENISE LTDS UMR 5513 CNRS, 58 rue Jean Parot, F42023 SAINT-ETIENNE

Résumé :

Cette contribution propose un modèle de milieu multi-phasique appliqué à l'étude de la peau humaine in vivo. La peau est considérée comme un milieu stratifié présentant trois couches (le stratum corneum, l'épiderme vivant et le derme) pour lequel les constituants présents sont trois solides, un fluide et des ions. Chaque couche est considérée comme un solide non-linéaire isotrope hyper-élastique de Mooney-Rivlin pouvant expérimenter de grands déplacements. Des simulations numériques sont présentées. La discussion permet de souligner l'aide de telles études pour obtenir des informations sur les propriétés mécaniques des différentes couches de la peau humaine in vivo.

Abstract :

This paper presents a tri-phasic model of skin in vivo. The skin is seen as a deforming stratified medium composed of three layers and made out of different fluid-saturated materials which contain also an ionic component. All the layers are treated as non-linear, isotropic Mooney-Rivlin materials. A new contact-free indentation device is presented. Example calculations are given. The numerical results correlate reasonably well with the typical observations of indented human skin. The discussion shows the versatility of this approach to obtain a better understanding on the mechanical behaviour of human skin layers separately.

Mots clefs : biomechanics, porous media, multi-phase media, fluid flow, human skin, transport of ions, indentation tests, Mooney-Rivlin material

1 Introduction

Human skin is the largest organ of the human body. It has a stratified structure consisting of four main layers: the stratum corneum, the viable epidermis, the dermis and the hypodermis. The skin protects the body against external influences by preventing fluid loss when exposed to sun, the penetration of undesirable substances in case of pollution and the development of diseases due to the direct application of external loads linked to clinical problems or aesthetic treatments. The state of this barrier (intact or damaged) governs its evolutions and its answers. Dryness, micro-cracks, loss of elasticity are thought to be influenced by fluid flow and the associated changes in ion concentration as a direct result of mechanical stress states. However, these phenomena are complex to understand and to model due to the strong couplings that exist between them and due to the complex behaviour of the different layers of skin tissues. Studies of the mechanical behaviour of human skin have shown that the skin is a stratified non-homogeneous, anisotropic, non-linear visco-elastic material which is subjected to a pre-stress in vivo [11] [12]. In addition its properties vary with age, throughout the body and per person. Difficulties arise when trying to obtain quantitative descriptions of mechanical properties of the skin. Numerous mechanical experiments have been performed on the skin: tensile testing, suction methods, torsion tests, indentation experiments. For in vivo performed mechanical experiments, the measured behaviour is generally ascribed to the dermis due to the relative height of the viable epidermis and of the stratum corneum [4] [5] [10]. However the various skin layers are tied together and it is hard to isolate the contribution of each of them. In vitro experiments give the opportunity to separate the skin layers. But in vitro experimental procedures change the mechanical properties of the individual skin layers. Moreover, it is hard to compare results obtained with different measurement conditions. This illustrates the need for an experimental system to measure the mechanical behaviour of the different skin layers in a non-invasive and objective manner and also independently of the experimental set-up. A new

experimental device is developed by the LTDS: a contact-free indentation tool able to give a better understanding of the mechanical behaviour of the skin by characterizing the mechanical behaviour of several distinct skin layers in vivo including for quite difficult experimental zones on the human body.

Within the framework of a general phenomenological thermo-hydro-mechanical and physico-chemical approach of heterogeneous media [8], a tri-phasic skin model is proposed in [1] [2] which incorporates a solid phase with three solid materials, a fluid phase and an ionic component under ambient constant conditions with no electrical effects. In this model, skin is considered as a stratified material with three layers modelling the three outer layers of skin: the stratum corneum, the viable epidermis and part of the dermis. These three layers are modelled separately in order to win insights on their own contribution to the overall response of the skin. All layers of the skin model are supposed to be made of fluid-saturated materials. Furthermore each layer is seen as a different solid material within the solid phase and it is described by its own behaviour law. In [3] the solid material is seen as an isotropic linear elastic material. In [2] the solid material is modelled as a non-linear isotropic Mooney-Rivlin material with one material constant. These models are able to describe the transient water flow and ion flow through skin after application of a saline solution and to gain insight on the mechanical behaviour of human skin layers separately. This paper proposes an extension of this skin model. Now the solid materials are seen as non-linear isotropic Mooney-Rivlin material with two material constants able to face large deformations.

To provide a proper setting, we will first recapitulate the governing equations for a deforming porous medium including ions and studied under quasi-static conditions. The non-invasive experimental device is presented. Then, example calculations for a specimen of skin are given and the obtained numerical results are discussed. Finally, some concluding remarks are made.

2 Theoretical model

Skin is seen here as a tri-phasic material with three solids for the solid phase ($\pi = s_1, s_2, s_3$), one for each layer, a fluid ($\pi = f$) and an ionic component ($\pi = i$), subjected to the restriction of no mass transfer and no chemical reactions between the constituents, the electrical effects are not taken into account and the components will be considered as intrinsically incompressible. In addition, the studied processes occur isothermally. With these assumptions, the balance of mass for each constituent π read:

$$\frac{\partial}{\partial t} \rho_\pi + \nabla \cdot \rho_\pi v_\pi = 0 \quad \text{for } \pi = s_1, s_2, s_3, f, i \quad (1)$$

with ρ_π relative mass density of constituent π , v_π absolute velocity of constituent π . As in the remainder of this paper, the subscripts s_1, s_2, s_3, f and i denote the solids, the fluid and the ions respectively. Neglecting inertia forces, convective terms and the gravity acceleration, the balance of linear momentum for each constituent π reduce to:

$$\nabla \cdot \sigma_\pi + p'_\pi = 0 \quad \text{for } \pi = s_1, s_2, s_3, f, i \quad (2)$$

with σ_π the Cauchy stress tensor of constituent π , p'_π the source of momentum for constituent π from the other constituents which takes into account the possible local drag interactions between the solids, the fluid and the ions and which satisfies the momentum production constraint: $p'_{s_1} + p'_{s_2} + p'_{s_3} + p'_f + p'_i = 0$. Under the assumption of chemically inert fluid and ions and with solid matrix materials, the material state relations expressing the chemical potentials of the fluid μ_f and of the ions μ_i encompass the interactions between solids, fluid and ions. For the fluid and the ion, the chemical potentials read

$$\mu_f = p - \Pi + \psi \quad \text{and} \quad \mu_i = \mu_{i0} + \frac{RT}{\bar{V}_i} \ln(c_i) \quad (3)$$

with p the fluid pressure, ψ the matrix potential accounting for fluid-solid interactions (capillary and adsorptive effects), Π the osmotic pressure accounting for fluid-ions interactions, μ_{i0} chemical potential of the ions in a reference state, R the universal gas constant, T the absolute temperature, c_i the concentration of the ions per unit fluid volume, \bar{V}_i partial molar volume of the ions. Neglecting couplings between velocity and heat flux, fluid flow through a saturated porous medium with ions is expressed by a generalized Darcy's law here under defined in terms of the fluid and ions chemical potentials and a second-order permeability tensor K

$$n_f v_f - v_s = -K \cdot \nabla \mu_f + \frac{n_i}{n_f} \nabla \mu_i \quad (4)$$

where n_π is the volumic ratio of constituent π defined by $\rho_\pi = n_\pi \rho'_\pi$ with ρ'_π absolute mass density of constituent π . Further, the sum of volumic ratios over the constituents present in the medium equals 1. The diffusion of ions through the fluid phase of the porous medium is taken into account through a Fick's law-type relation by means of a second-order diffusion tensor of the ions D_i

$$n_i v_i - v_f = -D_i \nabla \mu_i \quad (5)$$

The stress is, as usual, composed of a solid and a fluid part

$$\sigma = \sigma_{s1} + \sigma_{s2} + \sigma_{s3} - pI \quad (6)$$

with I the second-order identity tensor. The following scenarios were investigated for the stress-strain relations for the solids ($\pi = s_1, s_2, s_3$).

Analysis 1: Under the assumption of small displacements and small strains, skin is considered as a linear isotropic elastic material and a Hooke stress-strain relation is taken for each solid ($\pi = s_1, s_2, s_3$)

$$\sigma_\pi = D_\pi^e : \varepsilon_\pi \quad \text{and} \quad \varepsilon_\pi = \nabla^s u_\pi \quad \text{for } \pi = s_1, s_2, s_3 \quad (7)$$

where D_π^e is the elasticity tensor of the solid material π , ε_π is the strain tensor of solid π , u_π the displacement field of solid π and the superscript s denoting the symmetric part of the gradient operator.

Analysis 2: The assumption of small displacements and small strain is released. Skin is now seen as a non-linear isotropic hyper-elastic material able to face large deformations. A Mooney-Rivlin type stress-strain relation is considered for each solid ($\pi = s_1, s_2, s_3$)

$$\sigma_\pi = \alpha_1 B + \alpha_2 B^{-1} - p_1 I \quad (8)$$

where α_1 and α_2 are scalar functions, p_1 is the hydrostatic pressure, B is the left Cauchy-Green strain tensor of solid π defined versus the deformation gradient tensor F by $B = F F^T$. For incompressible, non-linear and isotropic materials, the stress can be expressed in terms of a strain energy function $W = W_\pi(I_1, I_2, I_3)$ where I_1, I_2 and I_3 are the scalar principal strain invariants of the right Cauchy-Green strain tensor $C = F^T F$ of solid π

$$I_1 = \text{tr } C \quad I_2 = \frac{1}{2} \text{tr}(C)^2 - \text{tr}(C^2) \quad I_3 = \det(C) \quad (9)$$

The second Piola-Kirchhoff stress tensor K of solid π can be elaborated as follows

$$K = 2 \frac{\partial W}{\partial C} = 2 \frac{\partial W}{\partial I_1} I + 2 \frac{\partial W}{\partial I_2} (I_1 I - C) + 2 \frac{\partial W}{\partial I_3} I_3 C^{-1} \quad (10)$$

leading to the following expression for the Cauchy stress tensor σ_π of solid π

$$\sigma_\pi = \frac{2}{j} \frac{\partial W}{\partial I_1} B - \frac{\partial W}{\partial I_2} (I_3 B^{-1} - I_2 I) + \frac{\partial W}{\partial I_3} I_3 I \quad (11)$$

The strain energy density function W for solid π is given as:

$$W = C_{10} I_1 - 3 + C_{01} I_2 - 3 + C_{11} I_1 - 3 I_2 - 3 + C_{20} I_1 - 3^2 + \dots + p_h (I_3 - 1) \quad (12)$$

where C_i, \dots are experimentally determined material constants of solid π and p_h is the hydrostatic pressure of solid π due to incompressibility. The last term of the strain energy density function W is the energy contribution from hydrostatic pressure and it is equivalent to zero for incompressible materials. In the proposed model, all layers are supposed to be made of intrinsically incompressible material. Therefore, the strain energy density function W reduces to

$$W = C_{10} I_1 - 3 + C_{11} I_1 - 3 (I_2 - 3) \quad (13)$$

Replacing in the Cauchy stress tensor expression (11) and taking into account that for incompressible hyper-elastic material $I_3 = 1$ and $j = 1$ yield

$$\sigma_\pi = 2 C_{10} + C_{11} I_2 - 3 C_{11} B - 2 C_{11} I_1 - 3 B^{-1} + 2 I_2 I \quad (14)$$

Equation (14) describes the relation between the Cauchy stress tensor and the left Cauchy-Green tensor and its invariants. This relation will be used to describe the mechanical behaviour of the different skin layers.

Analysis 3: Under the assumption that the model can simulate small displacements produced by pressures up to 10% of the experimentally applied pressure during contact-free indentation tests, the second term in the expression (13) of the strain energy function W can be neglected. The strain energy function then reduces to

$$W = C_{10} I_1 - 3 \quad (15)$$

Replacing in the Cauchy stress tensor expression (11) and taking into account that for incompressible hyper-elastic material $I_3 = 1$ and $j = 1$ yield

$$\sigma_\pi = 2 C_{10} B \quad (16)$$

This relation (16) will be used (Analysis 3) to describe the mechanical behaviour of the different skin layers. In this case, only three material parameters need to be identified: C'_{10s1} for the stratum corneum, C'_{10s2} for the viable epidermis and C'_{10s3} for the studied part of the dermis. The initial value problem is complemented with boundary conditions which hold on complementary parts of the boundaries of the different constituents. The initial value problem need also to be complemented with initial conditions.

3 Experimental device

The new indentation device developed by the LTDS is a contact-free indentation tool which permits to study in vivo the mechanical response of the human skin without pre-stressing it before the experiments. This contact-free indenter does not need to be fixed to the skin all along the test. It loads the skin mechanically by applying a controlled air flow onto the surface of the skin. Therefore it preserves the skin's natural state of stress. Moreover it is able to study quite difficult experimental zones on the human body. The experimental set-up is presented figure 1. Once the technician has programmed the order of magnitude of the applied load, the air flow entering in the indentation tool is controlled in diameter by the rotameter, released by the solenoid valve and then applied onto the surface of the skin. The penetration depth of the air flow is measured with a laser and recorded with a camera. A typical recorded curve for a contact-free indentation test performed on the volar forearm of a volunteered healthy adult is given in figure 1. The air flow (diameter 2 mm) is applied at a distance 10 mm from the surface of the skin. These experimental data are worked out and used in the numerical simulation, here after, to define physically admissible boundary and initial conditions and to help characterizing in vivo equivalent mechanical parameters of human soft tissues.

4 Numerical simulation

A finite difference analysis has been carried out. It allows a quantitative understanding of water and ion transport through skin and of deformations of the skin layers. The spatial derivatives in the field equations, i.e. the balance of momentum (2) for constituents $\pi=s_1, s_2, s_3, f, i$, the balance of mass (1) for the fluid $\pi=f$ and the balance of mass (1) for the ions $\pi=i$ are approximated with a second-order accurate finite difference scheme. Explicit forward finite differences are used to approximate the temporal derivatives, which are first-order accurate. As implied in the field equations, the velocities of the solids, the fluid and the ions are taken as fundamental unknowns and the displacements are obtained by integration when needed. All calculations are carried out for a specimen of skin with a depth of 0.156 mm at an ambient temperature of 21°C. This depth of the specimen of skin is taken as mean value typical for biological soft tissues available in the literature. The thickness is assumed to be uniform within each layer. The tissue composite consists of 40 elements. For the simulation, the model needs to be complemented by a set of material parameters [1] except as regards of the mechanical parameters for which a mechanical parameters estimation procedure is carried out. For the solid materials, the Young moduli (analysis 1) $E_{s1} = 2.0E7$ Pa, $E_{s2} = 3.0E2$ Pa, $E_{s3} = 2.0E3$ Pa are taken after [3]. For analysis 3, the material constants for the solids: $C'_{10s1} = 9.4E6$ Pa, $C'_{10s2} = 4.4E3$ Pa, $C'_{10s3} = 9.4E3$ Pa are taken after [2]. An absolute mass density $\rho' = 1330$ kg/m³ is assumed for each solid. For the fluid, an absolute mass density $\rho'_f = 1000$ kg/m³ is adopted. For the ions, an absolute mass density $\rho'_i = 7.5E-4$ kg/m³ is taken. In the calculations, the permeability $K = 1.98E-21$ m³/Ns and the diffusion coefficient $D_i = 3.3E-11$ m²/s are adopted. Boundary conditions for the upper skin surface are taken: an external compressive displacement $-3E-6$ m is applied at the upper skin surface simulating the air flow imposed by the contact-free indentation device, the skin surface is in contact with a 0.15 [M] NaCl solution. In the initial state, all layers are considered made out of fully saturated material with no ionic component. Therefore the volumic ratio of the ions is taken equal to zero for all the layers in the initial state.

5 Results and discussion

For analysis 2, the material constants for the solids ($C_{10s1} = 9.4E6$ Pa, $C_{11s1} = 8.2E7$ Pa), ($C_{10s2} = 4.4E3$ Pa, $C_{11s2} = 3.6E4$ Pa) and ($C_{10s3} = 9.4E3$ Pa, $C_{11s3} = 8.2E4$ Pa) are proposed. The numerical results are given in terms of profiles along the specimen of skin for 3 steps of calculations $t = 20s, 40s$ and $60s$ for analysis 1

(Hooke), analysis 2 (2 constants) and analysis 3 (1 constant). For the above sets of parameters, a zoom of the results for the volumic ratios of the ions and of the fluid are presented in figure 3. These results show a downward movement of the ions triggered by the applied mechanical and chemical external loads at the upper skin surface. The fluid volumic ratio of the skin surface changes almost immediately after a change in chemical potentials of the fluid and of the ions. The volumic ratio of deeper layers of the skin reacts more slowly. The results for the associated displacements of the solids are given in figure 4 and displayed a consolidation-type behaviour with negative displacements (initiated at the upper skin surface and extending to deeper layers) for the different layers of the skin tissues linked to the coupled downward fluid and ions fluxes initiated by the external applied loads and driven by the gradients of the fluid and ions chemical potentials which depend in their turn on the deformations of the solids. The numerical results obtained with the three analysis correlate reasonably well together. Comparison with results from the literature is not easy in case of non-linear material behaviour. The order of magnitude of these estimates for the material parameters taken for the simulations are coherent with the values reported by [1] [2] [10] [6] [7] respectively for the material constants of the stratum corneum and of the studied part of the dermis. As regards the viable epidermis, few data are available in the literature because skin is often seen as a one layer material or the viable epidermis is considered as part of the dermis [6] [7]. With the material parameters taken for the viable epidermis, the numerically obtained results lead to qualitatively equivalent mechanical answer of the overall skin when compared with the typical observations of indented human skin in vivo [7] [9] linked to the histology of the external skin layers. Stratum corneum is relatively thin (0.06 mm thick). However its dense coating of hard keratinized dead cells gives it a very strong tensile strength. The viable epidermis (0.1 mm thick) and the dermis (1-4 mm thick) are composed of softer living cells. The dermis is made up of collagen and elastin fibres embedded in ground substances. The dermis is thought to have a stronger strength than the thin viable epidermis made out of stratified squamous epithelial of soft keratinized living cells with nuclei.

6 Conclusion

Despite the large number of simplifications and assumptions, the tri-phasic skin model, composed of three solids, a fluid and an ionic component is able to describe the transient water flow and ion flow from skin in contact with a saline solution. Together with the numerical model presented here, they enable capturing deformations of the different layers of the skin composite separately. It offers perspectives for the investigation of skin barrier functions with non-invasive contact-free device in vivo.

References

- [1] Abellan M-A., Zahouani H., Feulvarch E., Bergheau J-M., Modelling water and ion transport through damaged skin, 2nd Euro-Mediterranean Conference on Bioengineering and Biomaterials (EMCBB), July 4-6, Fez, Morocco, 2012.
- [2] Abellan M-A., Feulvarch E., Zahouani H., Bergheau J-M., Contribution à la caractérisation expérimentale et simulation numérique du comportement de la peau humaine in vivo : indentation sans contact, 11^e Colloque National en Calcul des Structure (CSMA 2013), 13-17 mai, Giens, Var, 2013.
- [3] Abellan M-A., Feulvarch E., Bergheau J-M., Zahouani H., Coupled fluid flow and ion transport through intact skin, 38e Congrès de la Société de Biomécanique (SB 2013), 4-6 septembre, Marseille-Luminy, 2013.
- [4] Agache P., Monneu C., Lévêque J., De Rigal J., Mechanical properties and young's modulus of human skin in vivo. Archives of Dermatological Research, 269, 221-232, 1980.
- [5] Escoffier C., de Rigal J., Rochefort A., Vasselet R., Lévêque J., Agache P., Age-related mechanical properties of human skin : An in vivo study, The Journal of Investigative Dermatology, 93, 353-357, 1989.
- [6] Hendriks F.M.. Mechanical behaviour of human epidermal and dermal layers in vivo, Dissertation, Eindhoven University of Technology, 2005.
- [7] Hung A., Mithraratne K., Sagar M., Hunter P., Multilayer soft tissue continuum model: towards realistic simulation of facial expressions, World Academy of Science, Engineering and Technology, 54, 134-138, 2009.
- [8] Jouanna P., Abellan M-A., A generalized approach to heterogeneous media, Transport in Porous Media, 25, 351-374, 1996.
- [9] Leveque J.L., de Rigal J., Agache P.G., Monneur C., Influence of ageing on the in vivo extensibility of human skin at a low stress, Archives of Dermatological Research, 269 (2), 127-135, 1980.

- [10] Pailler-Mattei C., Bec C., Zahouani H., In vivo measurements of the elastic mechanical properties of human skin by indentation tests, *Medical Engineering and Physics*, 30, 599-606, 2008.
- [11] Rigal J D., Lévêque J., In vivo measurement of the stratum corneum elasticity, *Bioengineering and the Skin*, 1, 13-23, 1985.
- [12] Rochefort A., Propriétés biomécaniques du stratum corneum : - Modélisation rhéologique – Application à la cosmetology, Thèse de Doctorat, Université de Franche-Comté – Besançon, 1986.

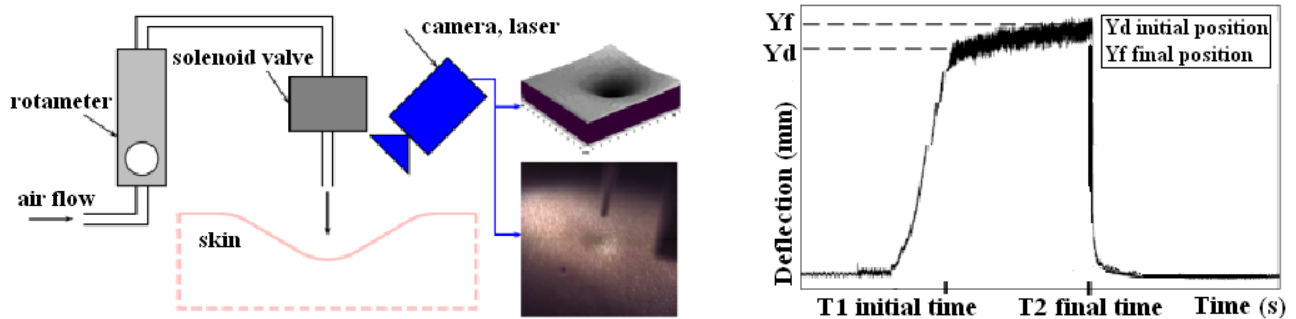


FIG. 1 - Experimental set-up (left) and recorded curve (right): the contact-free indentation device

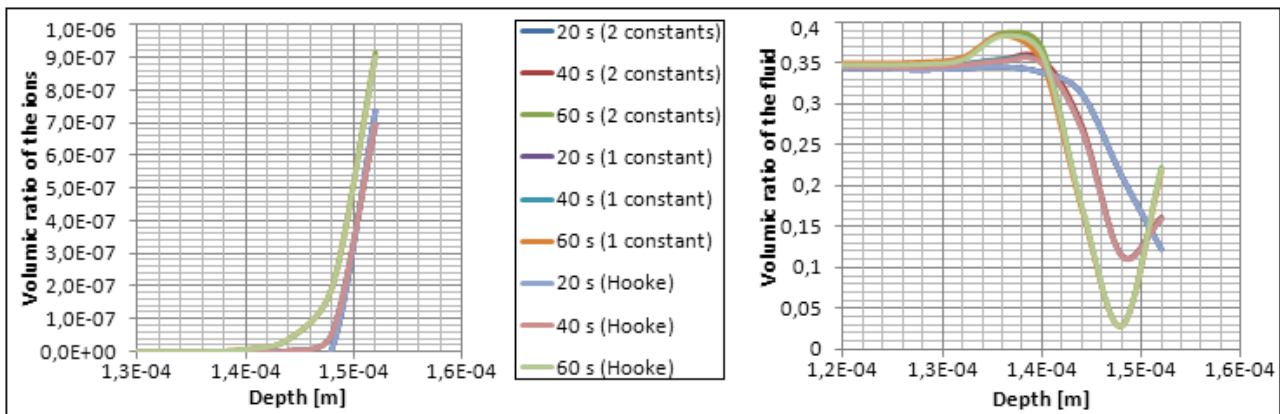


FIG. 3 – Zoom of the volumic ratios of the ions (left) and of the fluid (right): analysis 1 (Hooke), analysis 2 (2 constants) and analysis 3 (1 constant)

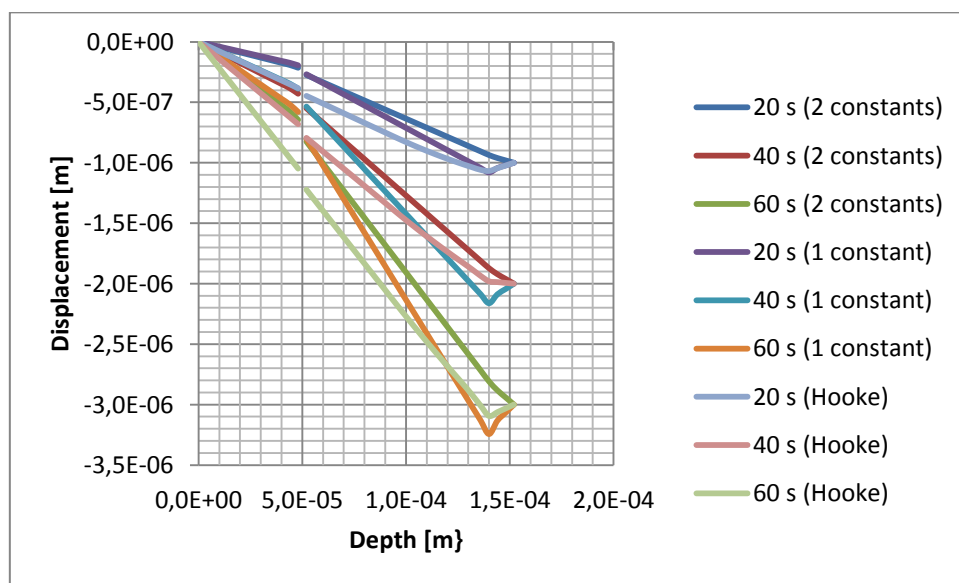


FIG. 4 – Downward displacements : analysis 1 (Hooke), analysis 2 (2 constants) and analysis 3 (1 constant)